ISBN: 978-3-95450-231-8 ISSN: 2673-5490 doi: 10.18429/JACoW-IPAC2023-THPM054

IMPACTS OF STRONGLY CURVED MAGNETIC MULTIPOLES ON COMPACT SYNCHROTRON DYNAMICS

H. X.Q. Norman[1,2] *, R. B. Appleby[1], University of Manchester, Manchester, UK
S. L. Sheehy [2], Australian Nuclear Science and Technology Organisation (ANSTO), Australia
E. Benedetto, SEEIIST Association, Geneva, Switzerland
[1] also at Cockcroft Institute, Warrington, UK
[2] also at University of Melbourne, Melbourne, Australia

Abstract

Superconducting curved magnets can reduce accelerator footprints by producing strong fields (>3 T) for applications such as carbon ion therapy, however the effect of strongly curved magnetic multipoles and fringe fields on accelerator beam dynamics is not fully understood. This is especially important for compact synchrotrons, where off-axis body fields and fringe fields can significantly affect beam quality and long-term beam stability. To establish the effect of magnet curvature on higher order multipole fields and on beam stability, an electromagnetic model of a superconducting, curved alternating- gradient canted-cosine-theta magnet (AG-CCT) is analysed. The magnet is studied for the main bending magnets in a 27 m circumference carbon ion therapy synchrotron, designed within the Next Ion Medical Machine Study (NIMMS) at CERN and the European project HITRIplus. The multipole fields of the magnet are implemented in a lattice model of the synchrotron in MAD-X/PTC to study long term beam stability, and to understand the effect of curved multipoles on particle dynamics for optimisation of both the lattice and magnet designs. Preliminary assessment of the performance of the synchrotron finds that the AG-CCT multipoles are well-tolerated in the lattice. Results are discussed for the suitability of the synchrotron for clinical application.

INTRODUCTION

Accelerator technology applied for charged particle therapy is being developed for future facilities. Emphasis is placed on reduction of physical footprints and power consumption to save costs and space for future facilities by generating stronger magnetic fields (>3 T) to accommodate for higher rigidity beams, such as carbon. From the clinical aspect, focus is placed on achieving higher intensity beams (1×10^{10} particles per extraction cycle) for more efficient treatment delivery.

This work focuses on one such design: a superconducting, compact (27 m circumference) carbon ion therapy synchrotron [1]. The synchrotron, designed within the European projects NIMMS and HITRIplus [2], is composed of four 90° canted-cosine-theta (CCT) magnets, with alternating-gradient (AG) focusing and defocusing quadrupole layers, operating at B_{main} = 3.5 T. The magnets are wound into two layers of two oppositely tilted helical coils, which produce high quality dipole fields and multipoles which are more easily adjustable [3] compared to other magnet types, e.g. cosine-theta (CT). The addition of curved AG-CCT magnets in the four bending sections reduces the physical size and weight of the accelerator from a typical normal conducting medical synchrotron circumference of 75 m [4], potentially leading to lower construction and operational costs due to requiring fewer magnets. It should be noted that an alternative layout of the lattice based on 60° CCT magnets also exists, as potential difficulties could arise when engineering the 90° bends [5].

In this paper we analyse the AG-CCT designed for the original NIMMS synchrotron using tools developed from studying a complementary curved (30°) combined-function CT magnet [6, 7]; numerical methods are used to extract multipole fields from field maps sampled from a model of the magnet using the EM magnet design software OPERA 3D [8]. The multipole fields and fringe fields of the AG-CCT are added to the sector bend magnets (SBENDS) of the accelerator lattice as thin lenses sandwiching the SBENDS, modelled in the beam optics codes MAD-X [9]/PTC [10] for particle tracking simulations, as represented in Fig. 1. We now refer to the field components as field **gradients**,

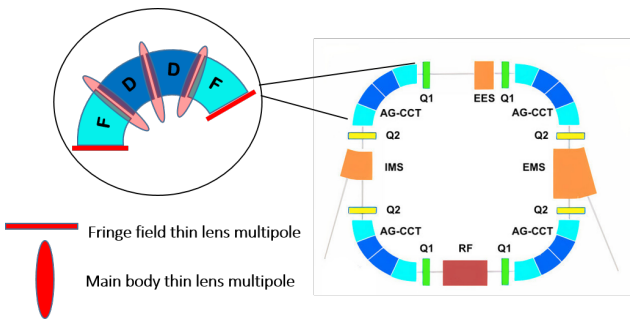

Figure 1: Layout of the original NIMMS synchrotron lattice. Inset: One of four 90° AG-CCT sector bends with fringe field and body field multipoles represented as thin lenses in the accelerator lattice in MAD-X.

as is used by beam dynamics codes. The reasoning is also that multipole decomposition is mathematically invalid for curved coordinate systems, further detailed in Ref. [11]. To understand the impact of introducing curvature and complex magnet geometry on long-term beam stability, 2×10^{10} carbon ions are simulated and tracked under the influence of higher order field gradients (i.e. sextupole and octupole).

* hannah.norman@manchester.ac.uk

ISBN: 978-3-95450-231-8 ISSN: 2673-5490 doi: 10.18429/JACoW-IPAC2023-THPM054

This indicates where stable tunes of operation are, as well as the size of the stable region in initial amplitude space: the dynamic aperture (DA). Plotting the DA enable visualisation of the maximum initial values of stable trajectories in (x, y) coordinate space in the lattice; ideally the DA should be as large as possible to allow for particle amplitude growth during acceleration while retaining the original beam. Valuable feedback can then provided to magnet and lattice designers for how much adjustment is required for the gradients before a prototype magnet can be developed for implementation in the medical synchrotron. Particles are first tracked through the gradients in the base lattice to approximate the DA without optimisation to investigate the tolerance of the lattice.

CURVED MAGNET ANALYSIS

OPERA 3D Model

The AG-CCT magnet is based on a similar design for a compact superconducting proton therapy gantry [12]; a custom magnet has been modified for the NIMMS synchrotron. The magnetic specifications are given in Table 1 in Ref. [1]. Due to the compactness of the magnets and synchrotron, it is crucial that the gradients are known, especially where the focusing-defocusing quadrupole layers overlap physically, and in the ends of the magnets where fringe fields will have significant effect [13]. The distribution of the field over the magnet and its individual sets of quadrupole and dipole layers is presented in Fig. 2.

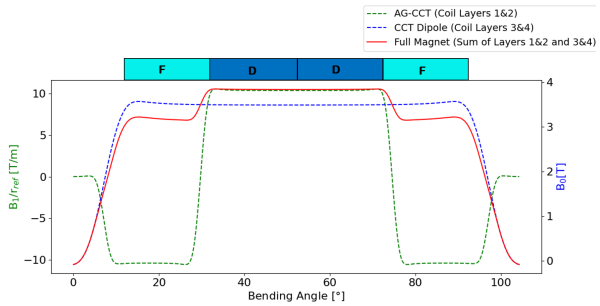

Figure 2: Main field B_z distributed over the magnet curvature (length). The separate dipole fields and quadrupole gradients are shown in addition to the sum of the fields between the four layers. r_{ref} is the reference radius, 2/3 the radius of the inner coil vacuum chamber (= 50 mm).

The presence of fringe fields and higher order gradients can drive resonances, leading to large tune shifts with amplitude of the beam over many turns in the accelerator. This leads to a reduction in DA and in turn reduce the uniformity of the beam spill, which would negatively impact the quality of treatment delivered to patients. The harmonic content of the magnet is analysed to assess if the gradients and fringe fields are within tolerable design limits. The main field is sampled along vectors perpendicular to a nominal trajectory through the magnet, approximated by two straight sections at the ends and an arc through the magnet centre following the curvature. A polynomial function is fitted to the main field along the magnet where there is mid-plane symmetry and the field is expanded to obtain the Taylor expansion coefficients [14]. From Fig. 2, there are three flattops (regions of constant field) corresponding to the locations of the focusing-defocusing quadrupole layers. We calculate the field gradients separately in these three locations and represent them as different 'gradient' lenses in the MAD-X lattice, as shown in Fig. 1. The external fringe fields are sampled both sides of the outermost flattops and integrated over the length of each fringe region to represent an overall 'kick' as a first approximation. Future studies will replace the kick with more lenses to better describe the individual fringe field contributions over those regions. One study has looked at the fewest number of gradient thin lenses that can accurately represent a magnet for tracking simulations; results are presented in Ref. [15]. The gradients calculated over the full magnet are given in Table 1. Work has been underway for translation of the AG-CCT field map into the ray-tracing code Zgoubi [16] to obtain a nominal trajectory from tracking through the 3D fieldmap directly to examine particle motion subject to the magnet curvature.

Table 1: AG-CCT integrated gradients B_n divided by a magnetic length for the fringe and body regions for rigidity $B\rho$ = 6.6 T m for a carbon ion beam at $E_{\text{kin,max}}$= 430 MeV/u. The gradients are calculated from polynomial fitting to the main field along the magnet mid-plane. Units for each order n are in T/(m^{n-1}).

Component	Outer Fringes	F-Layers	D-Layers
B_1 (Dip.)	2.50	3.3	3.93
B_2 (Quad.)	-7.26	-9.23	9.67
B_3 (Sext.)	2.80	3.1	5.42
B_4 (Oct.)	309.78	244.44	298.80

STABILITY STUDIES

Frequency Map Analysis

Particles on momentum were tracked through the lattice for 2048 turns; tracking parameters are the same as in Table 2 in Ref. [6], except for the normal working point, which has been moved away from extraction conditions to $Q_{x,y}$ = (1.72, 1.09). We first scan the initial (x, y) coordinate space up to the half-aperture ($A_{x,y}$=30 mm), as this has been deemed sufficient to accommodate the beam [1]. The fractional tunes $q_{x,y}$ are calculated for each coordinate using the NAFF algorithm [17]. This data was used to perform frequency map analysis (FMA) to establish the correspondence of initial particle trajectories in (x, y) amplitude space to stable tunes in the diagram [18], while identifying regions of resonance. The turn data is split into the first and last 1000 turns to calculate the tune diffusion index D from the RMS differences in $q_{x,y}$. From this data, resonant lines in tune space can be identified and the DA can be estimated from the stable region in (x, y) amplitude space.

ISBN: 978-3-95450-231-8 ISSN: 2673-5490 doi: 10.18429/JACoW-IPAC2023-THPM054

Positioning of Lattice Elements

Choice of gradient definition and positioning in the lattice is important. A common technique is to integrate the field gradients over an entire magnet and divide by an effective length to obtain average field gradients; it is insufficient to describe the field in this way for magnets with short lengths compared to the fringe field extent (e.g. the AG-CCT, ≈ 2 m in length). This is demonstrated in Fig. 3, where the DA is shown for tracking 1000 particles with sextupole fields distributed inside the SBENDS and represented as thin lens fringes. In this case, a reduction in DA is seen by distributing the gradients inside the SBENDS. With this representation, the individual contributions of the fields inside the magnet, which may give rise to non-linear particle behaviour, are erased. The gradients must be represented as several thin lenses over the magnet for accurate tracking results.

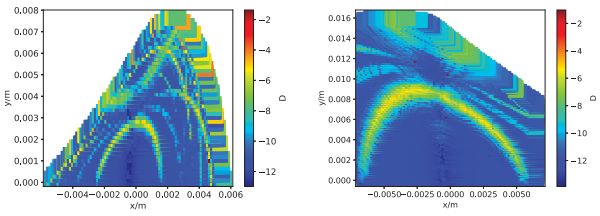

(a) (b)

Figure 3: Tune diffusion for (a) the sextupole field distributed inside each SBEND and (b) defined as thin lenses in the extremities of each bending magnet. Dark blue represents stable trajectories and dark red represents unstable trajectories, corresponding to initial amplitudes.

Tracking Results

The (fractional) tune space diagrams for the lattice with non-optimised gradients, under normal working conditions ($Q_{x,y}$ = 1.72, 1.09) and extraction conditions ($Q_{x,y}$ = 1.68, 1.13) are shown in Fig. 4. From Fig. 4, resonant tunes can be identified for the lattice with inclusion of gradients. While there are areas of instability present in Fig. 4(a), there is little

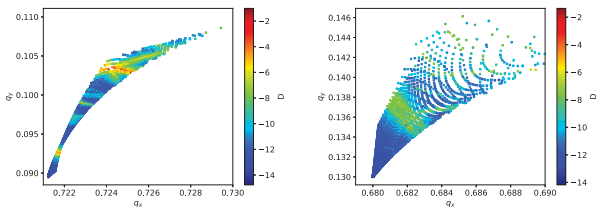

(a) (b)

Figure 4: FMA diagrams for inclusion of sextupole and octupole gradients for (a) $Q_{x,y}$ = (1.72, 1.09) and (b) $Q_{x,y}$ = (1.68, 1.13). Dark blue represents stable trajectories and dark red represents trajectories on unstable lines of resonance. White space indicates a particle has escaped.

overall tune spread; the gradients are small enough to not cause resonance crossing driving particle loss. Under extraction conditions in Fig. 4(b), there is larger tune spread, causing particle amplitude to grow outside the physical aperture for extraction. The DA can be estimated from the maximum (x, y) coordinates forming the hill shape in Fig. 5. The DA is calculated as $|x|$ = 0.013 m, $|y|$ = 0.006 m, compared with the base lattice without gradient lenses ($|x|$ = 0.014 m, $|y|$ = 0.010 m). As a preliminary investigation, the AG-CCT gradients are fairly well-tolerated in the synchrotron; the beam is not driven into resonance by the presence of the higher order fields. For this study, field contributions from transverse components B_x and B_y in the gradient calculations were not added for simplified calculations. Future studies will include the additional components to account for off-axis particle motion in the presence of non-linear fields produced by the magnet curvature.

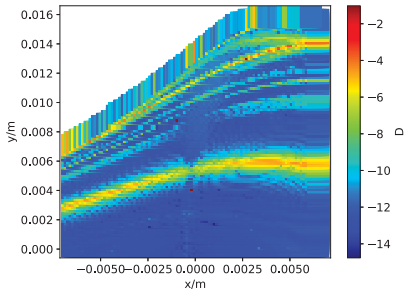

Figure 5: Tune diffusion diagram for inclusion of sextupole and octupole gradients for normal working conditions $Q_{x,y}$ = (1.72, 1.09).

OUTLOOK AND FUTURE WORK

This study was performed for tracking carbon ions at maximum therapeutic energy through realistic higher order field gradients from an AG-CCT magnet, designed for a compact superconducting synchrotron for carbon-ion therapy. Preliminary results show the gradients are tolerated by the synchrotron; non-linear effects are not being driven by the presence of the gradients to cause large tune shifts with initial particle amplitudes. A future study will look at tracking carbon ions through the AG-CCT in the synchrotron lattice in Zgoubi; results will be compared with this study to investigate margins of design error for the gradients in practice.

ACKNOWLEDGEMENTS

The authors would like to thank Lucas Brouwer and colleagues at Laurence Berkley National Laboratory for provision of an AG-CCT OPERA model designed for our studies; to Mikko Karpinnen at CERN for his provision of a CT OPERA model and additional support during analysis and to Ben Pine at Dassault Systèmes for his help and guidance in OPERA during this study. This work is supported by the Engineering and Physical Sciences Research Council (EPSRC) in the United Kingdom.

ISBN: 978-3-95450-231-8 ISSN: 2673-5490 doi: 10.18429/JACoW-IPAC2023-THPM054

REFERENCES

[1] E. Benedetto *et al.*, "A Carbon-Ion Superconducting Gantry and a Synchrotron Based on Canted Cosine Theta Magnets," *arXiv*, May 2021. doi:10.48550/arXiv.2105.04205.

[2] *Heavy Ion Therapy Research Integration (HITRIPlus) project website*, https://www.hitriplus.eu/.

[3] S. Caspi *et al.*, "Design, fabrication, and test of a superconducting dipole magnet based on tilted solenoids," *IEEE Transactions on Applied Superconductivity*, vol. 17, no. 2, pp. 2266–2269, 2007. doi:10.1109/TASC.2007.899243.

[4] L. Badano *et al.*, "Proton-Ion Medical Machine Study (PIMMS), 1," no. CERN-PS-99-010-DI, CERN-PS-99-010-DI, Mar. 1999.

[5] *The CERN-NIMMS Initiative and the SEEIIST Project, ICFA Slow Extraction Workshop 2022*, https://conference-indico.kek.jp/event/163/contributions/3146/attachments/2167/2712/EB_2022-01-24_nimmsSEEIIST_at_SXWorkshop.pdf.

[6] H. X. Q. Norman, R. B. Appleby, E. Benedetto, M. Karppinen, H. L. Owen, and S. L. Sheehy, "Performance Study of the NIMMS Superconducting Compact Synchrotron for Ion Therapy with Strongly Curved Magnets," in *Proc. IPAC'22*, (Bangkok, Thailand), Jul. 2022, pp. 3014–3017. doi:10.18429/JACoW-IPAC2022-THPOMS028.

[7] M. Karppinen, V. Ferrentino, C. Kokkinos, and E. Ravaioli, "Design of a curved superconducting combined function bending magnet demonstrator for hadron therapy," *IEEE Transactions on Applied Superconductivity*, vol. 32, no. 6, pp. 1–5, 2022. doi:10.1109/TASC.2022.3155537.

[8] *Opera | SIMULIA by Dassault Systèmes*, https://www.3ds.com/products-services/simulia/products/opera/.

[9] *MADX Manual*, https://mad.web.cern.ch/mad/.

[10] F. Schmidt, E. Forest, and E. McIntosh, "Introduction to the polymorphic tracking code: Fibre bundles, polymorphic Taylor types and "Exact tracking"," Tech. Rep. CERN-SL-2002-044-AP, KEK-REPORT-2002-3, Jul. 2002.

[11] D. Veres, T. Vaszary, E. Benedetto, and D. Barna, "A New Algorithm for Optimizing the Field Quality of Curved CCT Magnets," *IEEE Transactions on Applied Superconductivity*, vol. 32, no. 5, pp. 1–14, Mar. 2022. doi:10.1109/TASC.2022.3162389.

[12] W. Wan *et al.*, "Alternating-gradient canted cosine theta superconducting magnets for future compact proton gantries," *Phys. Rev. ST Accel. Beams*, vol. 18, p. 103 501, Oct. 2015. doi:10.1103/PhysRevSTAB.18.103501.

[13] S. Russenschuck, *Field computation for accelerator magnets: analytical and numerical methods for electromagnetic design and optimization*. Wiley, 2010. doi:10.1002/9783527635467.

[14] K. L. Brown, "A First and Second Order Matrix Theory for the Design of Beam Transport Systems and Charged Particle Spectrometers," *Adv. Part. Phys.*, vol. 1, no. SLAC-R-075, SLAC-75, pp. 71–134, 1968.

[15] L. Garolfi, E. Benedetto, and A. Latina, "Optics modeling of strongly curved magnets for compact synchrotron applications," 2023.

[16] F. Méot, "Ray-tracing code Zgoubi," *Nuclear Instruments and Methods in Physics Research, Section A: Accelerators, Spectrometers, Detectors and Associated Equipment*, vol. 427, no. 1-2, pp. 353–356, 1999. doi:10.1016/S0168-9002(98)01508-3.

[17] *GitHub- PyCOMPLETE/NAFFlib*, https://github.com/PyCOMPLETE/NAFFlib.

[18] J. Laskar, "Frequency map analysis and particle accelerators," vol. 1, Jun. 2003, 378–382 Vol.1. doi:10.1109/PAC.2003.1288929.